THE JOURNAL OF PHYSICAL CHEMISTRY C

ARTICLE

pubs.acs.org/JPCC

CO_2 Hydrogenation to Formic Acid on Ni(111)

Guowen Peng,[†] S. J. Sibener,[‡] George C. Schatz,[§] Sylvia T. Ceyer,[⊥] and Manos Mavrikakis*[,†]

[†]Department of Chemical and Biological Engineering, University of Wisconsin—Madison, Madison, Wisconsin 53706, United States

[‡]Department of Chemistry and The James Franck Institute, University of Chicago, Chicago, Illinois 60637, United States

[§]Department of Chemistry, Northwestern University, Evanston, Illinois 60208, United States

[⊥]Department of Chemistry, Massachusetts Institute of Technology, Cambridge, Massachusetts 02139, United States

ABSTRACT: Periodic, self-consistent, density functional theory (DFT) calculations are employed to study CO_2 hydrogenation on Ni(111). CO_2 hydrogenation with H adsorbed on the surface and with H absorbed in the subsurface is investigated systematically, and the respective microscopic reaction mechanisms are elucidated. We show that on Ni(111) CO_2 hydrogenation to formate intermediate is more favorable than to carboxyl intermediate. The hydrogenation to formate goes through the unidentate structure that rapidly transforms into the bidentate structure. Further hydrogenation from formate to formic acid is energetically more difficult than formate formation. Formation of adsorbed formic acid from adsorbed CO_2 and surface hydrogen is an endothermic reaction. Because subsurface H in Ni(111) is substantially less stable compared to surface H, its reaction with adsorbed CO_2 to adsorbed formic acid is an exothermic one. Our results may have significant implications for the synthesis of liquid fuels from CO_2 and for catalytic hydrogenation reactions in general.

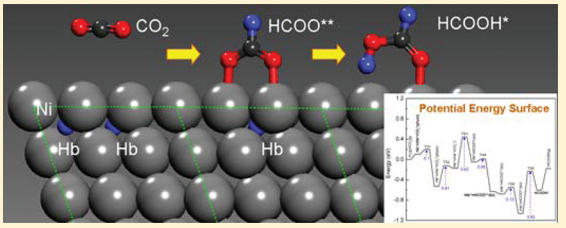

1. INTRODUCTION

Using CO_2 as a carbon source to synthesize useful chemicals is of great interest.[1,2] It is an abundant and inexpensive feedstock whose removal from industrial emissions is highly desirable to mitigate the greenhouse effect. One example of CO_2 conversion to a useful liquid hydrocarbon is hydrogenation of CO_2 to formic acid (HCOOH). Formic acid is an important chemical used in making animal feeds, in tanning and dyeing leather and textiles, and as a food preservative. Currently, formic acid synthesis is mainly performed through a two-step process: (1) the carbonylation of methanol to methyl formate ($HCOOCH_3$) using high pressures of toxic CO as the feedstock and (2) the hydrolysis of $HCOOCH_3$ to formic acid and methanol. Producing formic acid by direct hydrogenation of CO_2 is a promising alternate route in terms of economy, ecology, and safety. Thus, a detailed microscopic understanding on the reaction mechanism for CO_2 hydrogenation is of great importance.

Recently, Mavrikakis and co-workers studied CO_2 hydrogenation on Cu(111) and Pt(111) in the framework of their studies of the water gas shift (WGS) and its reverse reaction.[3,4] They found that formate, an intermediate involved in formic acid production, is a spectator species for the WGS reaction. The energy barriers for adding an adsorbed H atom to physisorbed CO_2 to form formate are 1.02 and 1.39 eV on Cu(111) and Pt(111), respectively. Using a mixture of CO_2, H_2, and CO over $Cu/ZnO/Al_2O_3$ catalysts, Chorkendorff and co-workers showed that Ni and Co significantly promote the rate of methanol production.[5,6] Because in the absence of the methanol synthesis gas phase environment and at typical reaction temperatures, Ni and Co would tend to segregate to the interior of Cu nanoparticles; the increase in activity was ascribed to a promotion through adsorbate-induced surface segregation of Ni and Co. Independently, Ni has been found to be a good catalyst for hydrogenation of hydrocarbons, whereby the presence of bulk and/or subsurface hydrogen played a special role in the observed reactivity.[7−10] In particular, it has been suggested that bulk and/or subsurface H exhibits unique reactivity in the heterogeneously catalyzed hydrogenation of hydrocarbons, such as methyl, ethylene, and acetylene, on Ni(111).[7−14] For example, in seminal work by Ceyer et al.,[7] it was unambiguously demonstrated that subsurface H is the reactant for hydrogenation of methyl radical to methane on Ni(111), whereas surface H is unreactive. The effect of subsurface species on the reactivity of transition metal surfaces was also found in other systems. For example, it has been shown that subsurface O increases the reactivity of Ag(111) toward dissociation of H_2, O_2, and NO[15] and oxidation of methanol.[16]

Very recently, it was reported that under ultrahigh-vacuum (UHV) conditions CO_2 can be hydrogenated to formate (HCOO) on Ni(110).[17] Further hydrogenation of HCOO to formic acid, however, was not observed. Under the UHV conditions applied in the work described in ref 17, only surface H exists on Ni. The absence of subsurface H under these experimental conditions may be the reason for the lack of formic acid production.

Here, we systematically study CO_2 hydrogenation with H adsorbed on the surface and with H absorbed in the subsurface on Ni(111). We explore the detailed reaction mechanism and derive the potential energy surface for CO_2 hydrogenation to formate and further to formic acid with surface H and subsurface H. We compare the competitive hydrogenation processes via

Received: October 29, 2011
Revised: December 22, 2011
Published: December 26, 2011

formate and carboxyl intermediates. We then discuss the role of subsurface H either as a spectator or as a reactant in CO_2 hydrogenation. Our results shed light on the microscopic reaction mechanism for CO_2 hydrogenation on Ni(111) in the absence and presence of subsurface H and may have significant implications for producing useful chemicals from CO_2.

2. COMPUTATIONAL METHODS

All calculations were performed using the Vienna ab initio Simulation Package (VASP) code[18,19] based on spin-polarized density functional theory. The projector augmented wave (PAW) potentials[20,21] were used for electron−ion interactions, and the generalized gradient approximation (GGA-PW91)[22] was used to describe the exchange-correlation functional. The electron wave function was expanded using plane waves with an energy cutoff of 400 eV. The Ni(111) surface was modeled by a five-layer slab with a (3×3) surface unit cell separated from its image in the z-direction by a vacuum equivalent of six atomic layers. The Brillouin zone of the Ni(111)-(3×3) surface was sampled using a $(4 \times 4 \times 1)$ k-point mesh based on the Monkhorst−Pack scheme.[23] The two bottom-most Ni(111) layers were fixed during relaxation. All structures were fully relaxed until the Hellmann−Feynman forces acting on the atoms were smaller than 0.05 eV/Å. Convergence with respect to energy cutoff, k-point set, and number of metal layers is confirmed. The climbing image nudged elastic band (CI-NEB) method[24] was used to calculate the activation energy barriers for the various elementary steps considered. Transition states were verified by calculating the Hessian matrix with the finite difference approach and identifying a single imaginary frequency.[25] The binding energy (BE) is defined as $BE = E_{ads} - E_{clean} - E_{gas}$, where E_{ads}, E_{clean}, and E_{gas} are the calculated total energies of the slab with adsorbate, the clean slab, and the adsorbate species in the gas phase, respectively. All calculations were performed with spin polarization, and a ferromagnetic phase was adopted for Ni(111), with a remaining magnetic moment of 0.67 μ_B per atom of the clean slab. The calculated Ni lattice constant is 3.52 Å, in good agreement with the experimental value of 3.524 Å.[26]

3. RESULTS AND DISCUSSION

A. Adsorption and Coadsorption of H and CO_2. We first studied the adsorption and coadsorption of atomic hydrogen (H) and CO_2 on Ni(111). The fcc hollow site is the most stable site (calculated binding energy of −2.83 eV) of a hydrogen atom adsorbed in an ordered (3×3) overlayer with a coverage of 1/9 monolayer (ML). The hcp hollow site is slightly less stable (by 0.01 eV), whereas the bridge and top sites are much less favorable, with binding energies of −2.69 and −2.22 eV, respectively. The calculated trends in binding of H on Ni(111) are in good agreement with results of earlier studies.[25,27] For CO_2 adsorption on Ni(111) at 1/9 ML coverage, we found that CO_2 is nearly parallel to the surface and the C−O bond length is 1.18 Å, which is nearly unchanged with respect to that in the gas phase CO_2 molecule. The z distance of CO_2 to the surface is ca. 3.5 Å. This adsorption geometry together with the weak calculated binding energy of −0.06 eV implies that CO_2 is weakly physisorbed on the surface, similar to what was found for CO_2 adsorption on Cu(111) and Pt(111).[3,4] The presence of 1/9 ML surface H at the fcc site of Ni(111) leaves the CO_2 adsorption geometry and binding energy practically unchanged.

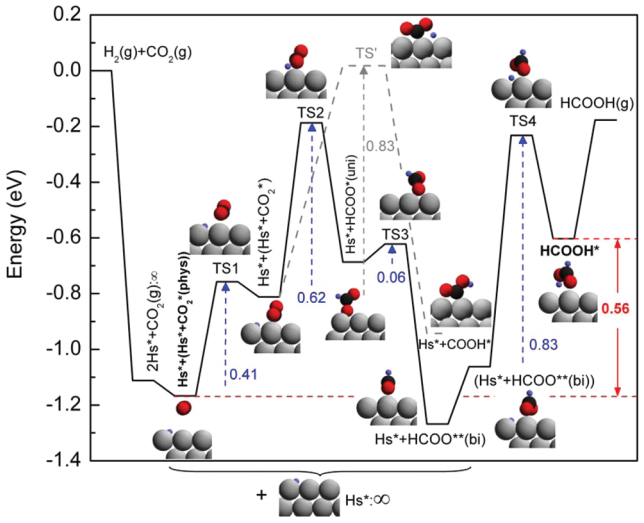

Figure 1. Potential energy surface (PES) of CO_2 hydrogenation to formate (HCOO) and formic acid (HCOOH) with H adsorbed (Hs*) on Ni(111). The dashed gray line shows the PES for CO_2 hydrogenation to carboxyl (COOH) intermediate. The atomic structures of reactants, intermediates, transition states, and products are schematically illustrated in the respective insets. Blue, black, red, and gray spheres indicate H, C, O, and Ni atoms, respectively. Asterisk denotes an adsorbed state. Two species within the same parentheses signify a coadsorbed state. TS represent transition states. Symbol ∞ denotes that adsorbed states at infinite separation from each other (no interaction energy).

This is expected because CO_2 is far away from the surface and the interaction with the adsorbed H is negligible.

B. CO_2 Hydrogenation with Surface H. Having analyzed the adsorption and coadsorption of H and CO_2, we then studied CO_2 hydrogenation on Ni(111). For CO_2 hydrogenation with H adsorbed on the surface (H_s), two different routes exist: CO_2 can be hydrogenated either at its carbon atom to lead to formate (HCOO) formation or at its oxygen atom to lead to carboxyl (COOH) formation, an intermediate that was proposed to be key for the low-temperature WGS reaction on Cu(111) and Pt(111).[3,4] On Ni(111), our calculations suggest that formate in its most stable bidentate structure (HCOO**(bi), with two O atoms bound to two Ni atoms at atop sites) is more stable than carboxyl (COOH) in its most stable trans configuration (with H pointing toward to the surface) by 0.32 eV. This is in contrast to the gas phase structures of these species, where COOH is more stable than HCOO by ∼0.4 eV.[28] We first examine CO_2 hydrogenation to formate. Shown in Figure 1 is the calculated potential energy surface (PES) for CO_2 hydrogenation to HCOOH via the formate intermediate. We found that before reacting with the adsorbed surface H to form formate, the physisorbed CO_2 moved close to the surface and settled in a metastable state characterized by a bent CO_2 geometry. In this metastable state, designated as (Hs* + CO_2*) in Figure 1, the C−O bond lengths are 1.21 and 1.26 Å, and the longer C−O bond is nearly parallel to a Ni−Ni bond. The O−C−O bond angle in that state is 138°. This metastable state is 0.36 eV less stable than the weakly physisorbed state and has been suggested as an intermediate state for CO oxidation on oxygen-predosed Ni(111)[29] and Pt(111).[30] The activation energy barrier of transforming the physisorbed state into the metastable state is 0.41 eV. In the transition state (see TS1 in Figure 1), the C−O bond lengths are 1.19 and 1.21 Å, and the O−C−O bond angle is 160°. After CO_2 reaches that

state on the surface, it is ready to react with the preadsorbed H and form formate. The minimum-energy path involves the approach of H to C en route to forming a H−C bond. The distance between H and C at the transition state (TS2 shown in the inset of Figure 1) is 1.29 Å, which is only 0.18 Å larger than the H−C bond length in the preferred adsorbed state of formate. After that, the molecule flips and ends up with formate in a unidentate structure with one of its O atoms positioned at an fcc site (state denoted as (HCOO*(uni), thereafter). The activation energy barrier for this reaction is 0.62 eV. Notice that the unidentate formate is 0.59 eV less stable than the bidentate structure, which has both its O atoms bonded to two Ni atoms at atop sites. A similar unidentate formate was found to be stable on Cu(111)[3] but not on Pt(111).[4] The transformation from the unidentate to the bidentate formate is almost spontaneous, with a very small barrier of 0.06 eV. This is similar to the respective formate structural transformation on Cu(111).[3] We also analyzed the minimum-energy path for hydrogenation from the coadsorbed CO_2 and surface H state directly to the bidentate formate, without passing through the unidentate structure. Compared with the two-step process path (via the unidentate formate) which needs an overall energy barrier of 0.62 eV, the direct path, not shown in Figure 1, is characterized by an energy barrier of 0.78 eV and is, therefore, less favorable.

We now consider the other route for CO_2 hydrogenation on Ni(111) that adds the H atom to one of the two oxygen atoms of CO_2 and leads to the carboxyl (COOH) intermediate. Similarly to the microscopic findings for formate formation, we found that for carboxyl formation the physisorbed CO_2 state transforms to the metastable CO_2 state first as discussed above. The resulting CO_2 state reacts with the coadsorbed surface H atom to from carboxyl in its most stable *trans* configuration. The relevant energetics is shown with the gray dashed line in Figure 1. The activation energy barrier to form carboxyl is 0.83 eV, which is 0.21 eV higher than the barrier to form formate. The inferior thermochemical stability of carboxyl relative to formate and the higher activation energy barrier associated with carboxyl formation suggest that the hydrogenation route via formate is clearly favored on Ni(111). Therefore, we will not consider the carboxyl route further for the purpose of this study.

We then turn our attention to adding a surface H atom to formate to produce a formic acid molecule on the Ni(111) surface. First, we find that there is a repulsive interaction (∼0.2 eV) between coadsorbed HCOO(bi) and H (see Table 1). For the adsorption of the final product formic acid on Ni(111), we found that the most stable site is the atop site, with O of the carbonyl bonding with an atop Ni atom and the OH being above a bridge site. The PES of the second hydrogenation to form formic acid is also provided in Figure 1. The respective reaction coordinate involves HCOO rotation toward H and diffusion of H from the fcc site to the neighboring bridge site for the final H−O bond making event. At the transition state (TS4 shown in Figure 1), the O−H distance is 1.49 Å. After the TS, H moves vertically toward O (of C═O) and settles with HCOOH in the atop molecular structure. As shown, an activation energy barrier of 0.83 eV is associated with this second hydrogen addition step. This barrier is larger than that of the first hydrogen addition step (0.62 eV), indicating that the second hydrogenation step might be the rate-determining step for formic acid production.

C. CO_2 Hydrogenation with Subsurface H. As discussed above, subsurface and bulk hydrogen in metals, such as Ni, have been shown to possess substantially different reactivity than surface-adsorbed hydrogen in the catalytic hydrogenation of hydrocarbons.[11,12] Subsurface and bulk H could act as spectators modifying the electronic structure of the metal surface, and thus its catalytic activity,[31] or act as a direct reactant in the hydrogenation reaction.[7] Compared to surface H, subsurface H in the octahedral site (O_h) of Ni(111)—directly underneath a surface fcc site—is metastable, with a binding energy of −2.19 eV. This metastable subsurface H can be prepared at low temperatures by exposure of the surface to atomic hydrogen followed by collision-induced recombinative desorption to remove the surface bound H under UHV conditions.[32−34] To explore the role of subsurface H (H_b) in CO_2 hydrogenation on Ni(111), we first studied CO_2 hydrogenation with surface H in the presence of subsurface H as a spectator. We then studied CO_2 hydrogenation with subsurface H as a reactant at a low coverage (2/9 ML) and a full ML coverage.

Table 1. Binding Energy (in eV) of CO_2, HCOO, and HCOOH on Clean Ni(111), Ni(111) with a 1/9 Monolayer (ML) Surface H (H_s), and a 1/9 ML as Well as 1 ML Subsurface H (H_b)[a]

adsorbate	site	clean	1/9 ML H_s	1/9 ML H_b	1 ML H_b
CO_2	physisorbed	−0.06	−0.06	−0.06	−0.06
	metastable state	+0.19	+0.30	+0.27	+0.21
HCOO	unidentate	−2.45		−2.46	−2.30[b]
	bidentate	−3.03	−2.84	−3.13	−3.00[b]
HCOOH	atop	−0.43		−0.48	−0.48[c]

[a] Binding energies refer to the respective adsorbates in the gas phase. [b] The coverage of H_b is 8/9 ML. [c] The coverage of H_b is 7/9 ML.

In the study of CO_2 hydrogenation with surface H in the presence of subsurface H as a spectator species, one H atom is preabsorbed at an O_h site in the first subsurface layer of Ni(111), corresponding to a H_b coverage of 1/9 ML. The elementary steps of the reaction along the path shown in Figure 1 were all recalculated, and the results are shown in Figure 2. By comparing Figure 1 with Figure 2, we conclude that within the accuracy of our calculations subsurface H as a spectator species does not change the PES of CO_2 hydrogenation with surface H. Hence, the effect of subsurface H as a spectator on the reactivity of the Ni(111) surface toward CO_2 hydrogenation is small and can be neglected.

Next, we investigated CO_2 hydrogenation with subsurface H in Ni(111) as a reactant. We started with the initial structure with a subsurface H at an O_h site and a CO_2 physisorbed at the surface. The PES we found for CO_2 hydrogenation using the subsurface H as a reactant is shown in Figure 3. The presence of the preabsorbed subsurface H has negligible effect on CO_2 adsorption. The calculated binding energy of physisorbed CO_2 is essentially unchanged (see Table 1). For the reaction between subsurface H and physisorbed CO_2 to happen, subsurface H has to emerge onto the surface and physisorbed CO_2 has to move closer the surface. Our CI-NEB calculations using the structure with subsurface H at an O_h site and physisorbed CO_2 as the initial state and a final state comprised of an H atom at an fcc site and a CO_2 molecule in its metastable surface state discussed above showed that the subsurface H emergence onto the surface occurs before the transformation of the physisorbed CO_2 into its surface metastable state. The emergence of subsurface H is characterized by an activation energy barrier of 0.1 eV. At the transition state of H emergence, the interatomic distance between the surface Ni

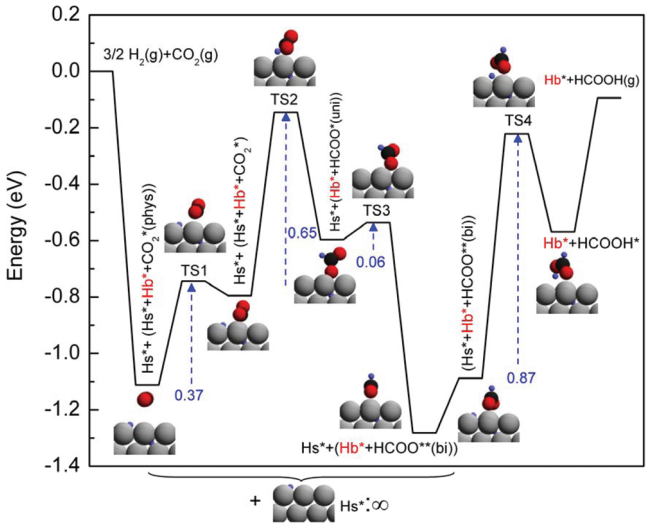

Figure 2. Potential energy surface of CO_2 hydrogenation to formate (HCOO) and formic acid (HCOOH) with surface H (Hs*) at 2/9 ML initial coverage on Ni(111) and in the presence of 1/9 ML subsurface H (Hb*) as a spectator species. The detailed structures of reactants, transition states, intermediates, and products are schematically illustrated in insets. For further symbol definitions see caption of Figure 1.

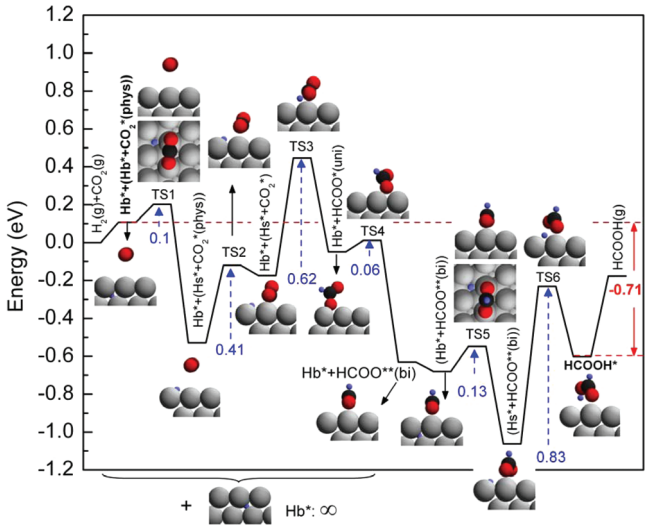

Figure 3. Potential energy surface of CO_2 hydrogenation to formate (HCOO) and formic acid (HCOOH) on Ni(111) with 2/9 monolayer subsurface H as the initial reactant. The atomic structures of reactants, transition states, intermediates, and products are schematically illustrated in insets. For symbol definitions, see Figure 1.

atoms surrounding the emerging H atom is ca. 5% larger than the equilibrium distance in Ni(111), and the H atom is nearly at the same height as its neighboring Ni atoms. After the emergence of subsurface H to the surface, the reaction paths of the transformation from physisorbed CO_2 to the metastable state of surface CO_2 and the first hydrogenation to formate using the emerged H as a reactant are exactly the same as in the corresponding steps of CO_2 hydrogenation with surface H (see earlier discussion).

By introducing a second subsurface H coadsorbed with a HCOO in its bidentate state, we studied the second hydrogenation leading from formate to formic acid. The presence of the

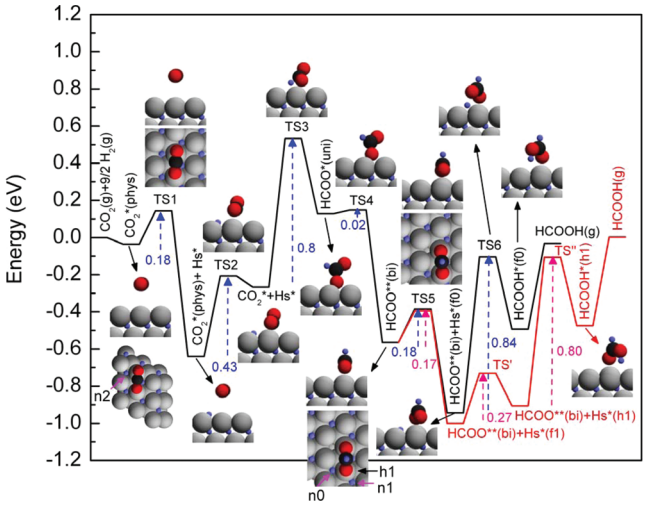

Figure 4. Potential energy surface of CO_2 hydrogenation to formate (HCOO) and formic acid (HCOOH) on Ni(111) with a full monolayer of subsurface H. The atomic structures of reactants, transition states, intermediates, and products are schematically illustrated in insets. Pink solid arrows in insets denote the subsurface H (n_0, n_1, and n_2) which eventually emerge to the surface. See text for details and Figure 1 for symbol definitions.

subsurface H slightly stabilizes the adsorbed formate. As seen in Table 1, the binding energy of the bidentate formate is −3.13 eV, whereas it is −3.03 eV on the clean Ni(111). Our CI-NEB calculations suggest that, before reacting with the formate, the subsurface H emerges onto the surface, with an energy barrier of 0.13 eV. After emergence of the subsurface H atom, the pathway for the hydrogenation of formate to formic acid is the same with that described above (0.83 eV activation energy barrier).

We notice that the metastable subsurface H changes the thermochemistry of the overall reaction $2H^* + CO_2^* \rightarrow HCOOH^*$. As shown in Figures 1 and 3, the reaction $2H_s^* + CO_2^* \rightarrow HCOOH^*$ is endothermic by 0.56 eV, whereas the reaction $2H_b^* + CO_2^* \rightarrow HCOOH^*$ is exothermic by 0.71 eV. This difference reflects the energy difference between two surface and two subsurface H atoms on/in Ni(111). Unfortunately, the methods used in this work do not allow directly probing reactivity of the emerging H atom with the metastable CO_2 surface state before the emerging H atom has equilibrated with the surface and become a surface bound H atom. We are currently exploring that reactivity by utilizing the appropriate force-fields-based Born−Oppenheimer molecular dynamics calculations.

Finally, we studied CO_2 hydrogenation on Ni(111) with a full ML of H absorbed in the first subsurface layer, which is the model system representing reactivity of Ni(111) loaded with subsurface H by using the collision-induced recombinative desorption strategy.[7,32−34] The most stable configuration has all O_h sites in the subsurface populated with H. At a full ML coverage, the calculated binding energy is −2.27 eV per subsurface H, which is slightly larger (by 0.08 eV) in magnitude than that in a low coverage limit discussed earlier. This indicates that the interaction between absorbed subsurface H is attractive. To explore the hydrogenation process on Ni(111) with a full ML H_b, we first calculated the adsorption of a CO_2 molecule on the surface. As on clean Ni(111), we found that CO_2 is weakly physisorbed on the surface and the presence of H_b does not change its binding strength. The overall PES for CO_2 hydrogenation on Ni(111) with 1 ML subsurface H is shown in Figure 4.

dx.doi.org/10.1021/jp210408x |J. Phys. Chem. C 2012, 116, 3001–3006

Similarly to CO_2 hydrogenation with H_b as a reactant at low coverage, we found that the interaction of newly emerged H_b with adsorbed CO_2 results in movement of CO_2 closer to the surface, leading to the metastable ($Hs^* + CO_2^*$) state. The emergence of the Hb from site n_2 (see inset in Figure 4) to the corresponding surface fcc site is characterized by a 0.18 eV activation energy barrier. Following the emergence of H_b, the weakly physisorbed CO_2 comes close to the surface and goes to its metastable state with an energy barrier of 0.43 eV. Subsequently, the first hydrogenation step $H_s^* + CO_2^* \rightarrow$ HCOO* (uni) is characterized by a 0.8 eV energy barrier, which is 0.18 eV larger than that the corresponding barrier on the clean Ni(111). The subsequent transformation HCOO*(uni) $\rightarrow$ HCOO**(bi) takes place almost spontaneously. To study the second hydrogenation from HCOO**(bi) to formic acid HCOOH*, we considered two pathways using two different H_b at the nearest H_b at site n_0 and the next-nearest H_b at site n_1, as indicated by the pink arrows in the atomic structure of HCOO**(bi) shown in the inset of Figure 4. The first path for the second hydrogenation includes two steps: (1) the emergence of H_b at n_0 to the above fcc site (f_0), which has the same energy barrier (0.18 eV) as the first H_b emergence, and (2) the reaction between H_s at f_0 and HCOO**(bi), which requires an energy barrier of 0.84 eV, similar to the respective process at low H_b coverage. The second path for the hydrogenation to formic acid consists of three steps: (1) the emergence of H_b at n_1 to the fcc site right above (f_1), with an energy barrier of 0.17 eV, (2) the diffusion of H_s at f_1 to the neighboring hcp site h_1 with an energy barrier of 0.27 eV, and (3) the reaction of H_s at h_1 and HCOO**(bi) with an energy barrier of 0.80 eV. Overall, the hydrogenation from CO_2^* to HCOOH* on Ni(111) with 1 ML H_b absorbed is exothermic with an reaction energy of −0.46 eV. The energy barriers for the first and second hydrogenation steps are comparable (∼0.8 eV).

4. CONCLUSIONS

In summary, we presented a periodic, self-consistent DFT study of CO_2 hydrogenation on Ni(111) surfaces. We systematically studied CO_2 hydrogenation with H adsorbed on the surface and with H absorbed in the subsurface. Our results showed that CO_2 hydrogenation to formate intermediate is more favorable than to carboxyl intermediate. The first hydrogenation to formate goes through the unidentate structure with a barrier of ∼0.6 eV, whose structure then transforms to the more stable bidentate structure easily. The second hydrogenation process from formate to formic acid is energetically more difficult than the first hydrogenation (barrier of ∼0.8 eV). Furthermore, we studied the role of subsurface H either as a spectator or as a reactant in CO_2 hydrogenation on Ni(111). We showed that subsurface H as a spectator essentially has no effect on the hydrogenation process. In contrast, subsurface H as a reactant by emerging out onto the surface changes the thermodynamics of CO_2 hydrogenation to adsorbed HCOOH from endothermic to exothermic, due to the excess energy possessed by the less stable subsurface H. Our studies have probed surface chemistry with H equilibrated on the Ni(111) surface upon its emergence from subsurface. Current studies explore the analogous chemistry on Ni(110) and other more direct reactive paths, where the transient nonequilibrated H species reacts with adsorbed CO_2 as it emerges from the subsurface.

AUTHOR INFORMATION

Corresponding Author
*E-mail: manos@engr.wisc.edu.

ACKNOWLEDGMENT

This work was supported by National Science Foundation through the Center for Energetic Non-Equilibrium Chemistry at Interfaces (Grant 0943639). CPU time was used at supercomputing resources located at EMSL, a National scientific user facility at Pacific Northwest National Laboratory (PNNL); the Center for Nanoscale Materials at Argonne National Laboratory (ANL); the National Center for Computational Sciences at Oak Ridge National Laboratory (ORNL); and the National Energy Research Scientific Computing Center (NERSC). EMSL is sponsored by the Department of Energy's Office of Biological and Environmental Research located at PNNL. CNM, NCCS, and ORNL are supported by the U.S. Department of Energy, Office of Science, under Contracts DE-AC02-06CH11357, DEAC05-00OR22725, and DE-AC02-05CH11231, respectively.

REFERENCES

(1) Leitner, W. *Angew. Chem., Int. Ed. Engl.* **1995**, *34*, 2207–2221.
(2) Jessop, P. G.; Ikariya, T.; Noyori, R. *Chem. Rev.* **1995**, *95*, 259–272.
(3) Gokhale, A. A.; Dumesic, J. A.; Mavrikakis, M. *J. Am. Chem. Soc.* **2008**, *130*, 1402–1414.
(4) Grabow, L. C.; Gokhale, A. A.; Evans, S. T.; Dumesic, J. A.; Mavrikakis, M. *J. Phys. Chem. C* **2008**, *112*, 4608–4617.
(5) Nerlov, J.; Chorkendorff, I. *J. Catal.* **1999**, *181*, 271–279.
(6) Nerlov, J.; Sckerl, S.; Wambach, J.; Chorkendorff, I. *Appl. Catal., A* **2000**, *191*, 97–109.
(7) Johnson, A. D.; Daley, S. P.; Utz, A. L.; Ceyer, S. T. *Science* **1992**, *257*, 223–225.
(8) Daley, S. P.; Utz, A. L.; Trautman, T. R.; Ceyer, S. T. *J. Am. Chem. Soc.* **1994**, *116*, 6001–6002.
(9) Haug, K. L.; Burgi, T.; Trautman, T. R.; Ceyer, S. T. *J. Am. Chem. Soc.* **1998**, *120*, 8885–8886.
(10) Haug, K. L.; Burgi, T.; Gostein, M.; Trautman, T. R.; Ceyer, S. T. *J. Phys. Chem. B* **2001**, *105*, 11480–11492.
(11) Kokes, R. J.; Emmett, P. H. *J. Am. Chem. Soc.* **1959**, *81*, 5032–5037.
(12) Kokes, R. J.; Emmett, P. H. *J. Am. Chem. Soc.* **1959**, *82*, 4497–4501.
(13) Michaelides, A.; Hu, P.; Alavi, A. *J. Chem. Phys.* **1999**, *111*, 1343–1345.
(14) Ledentu, V.; Dong, W.; Sautet, P. *J. Am. Chem. Soc.* **2000**, *122*, 1796–1801.
(15) Xu, Y.; Greeley, J.; Mavrikakis, M. *J. Am. Chem. Soc.* **2005**, *127*, 12823–12827.
(16) Millar, G. J.; Nelson, M. L.; Uwins, P. J. R. *J. Catal.* **1997**, *169*, 143–156.
(17) Vesselli, E.; De Rogatis, L.; Ding, X. L.; Baraldi, A.; Savio, L.; Vattuone, L.; Rocca, M.; Fornasiero, P.; Peressi, M.; Baldereschi, A.; Rosei, R.; Comelli, G. *J. Am. Chem. Soc.* **2008**, *130*, 11417–11422.
(18) Kresse, G.; Furthmüller, J. *Phys. Rev. B* **1996**, *54*, 11169–11186.
(19) Kresse, G.; Furthmüller, J. *Comput. Mater. Sci.* **1996**, *6*, 15–50.
(20) Blochl, P. E. *Phys. Rev. B* **1994**, *50*, 17953–17979.
(21) Kresse, G.; Joubert, D. *Phys. Rev. B* **1999**, *59*, 1758–1775.
(22) Perdew, J. P.; Wang, Y. *Phys. Rev. B* **1992**, *45*, 13244–13249.
(23) Monkhorst, H. J.; Pack, J. D. *Phys. Rev. B* **1976**, *13*, 5188–5192.
(24) Henkelman, G.; Uberuaga, B. P.; Jonsson, H. *J. Chem. Phys.* **2000**, *113*, 9901–9904.
(25) Greeley, J.; Mavrikakis, M. *Surf. Sci.* **2003**, *540*, 215–229.

(26) *CRC Handbook of Chemistry and Physics*, 76th ed.; CRC Press: New York, 1996.
(27) Greeley, J.; Krekelberg, W. R.; Mavrikakis, M. *Angew. Chem., Int. Ed.* **2004**, *43*, 4296–4300.
(28) Lakin, M. J.; Troya, D.; Schatz, G. C.; Harding, L. B. *J. Chem. Phys.* **2003**, *119*, 5848–5859.
(29) Peng, G. W.; Merte, L. R.; Knudsen, J.; Vang, R. T.; Lægsgaard, E.; Besenbacher, F.; Mavrikakis, M. *J. Phys. Chem. C* **2010**, *114*, 21579–21584.
(30) Alavi, A.; Hu, P. J.; Deutsch, T.; Silvestrelli, P. L.; Hutter, J. *Phys. Rev. Lett.* **1998**, *80*, 3650–3653.
(31) Ferrin, P. A.; Kandoi, S.; Zhang, J. L.; Adzic, R.; Mavrikakis, M. *J. Phys. Chem. C* **2009**, *113*, 1411–1417.
(32) Johnson, A. D.; Maynard, K. J.; Daley, S. P.; Yang, Q. Y.; Ceyer, S. T. *Phys. Rev. Lett.* **1991**, *67*, 927–930.
(33) Ceyer, S. T. *Acc. Chem. Res.* **2001**, *34*, 737–744.
(34) Maynard, K. J.; Johnson, A. D.; Daley, S. P.; Ceyer, S. T. *Faraday Discuss.* **1991**, *91*, 437–449.